ELSEVIER

Available online at www.sciencedirect.com
ScienceDirect

Journal of Catalysis 247 (2007) 68–77

JOURNAL OF CATALYSIS

www.elsevier.com/locate/jcat

Copper oxide and niobium pentoxide supported on silica-alumina: Synthesis, characterization, and application on diesel soot oxidation

Valdeilson S. Braga, Fillipe A.C. Garcia, José A. Dias *, Sílvia C.L. Dias *

Universidade de Brasília, Instituto de Química, Laboratório de Catálise, Caixa Postal 4478, Brasília-DF 70904-970, Brazil

Received 19 October 2006; revised 16 December 2006; accepted 30 December 2006

Abstract

Copper oxide and niobium pentoxide were supported on silica-alumina by two methods: co-impregnation and sequential impregnation, with CuO:Nb_2O_5 ratios of 1:10 and 1:1. These new materials showed different characteristics according to the preparation method. The copper and niobium precursors totally decomposed after treatment at 300 °C for 6 h. The materials prepared by sequential impregnation exhibited lower thermal stability than the analogous ones prepared by co-impregnation based on the Nb_2O_5 transition phase. Whereas that transition occurs at about 1356 °C in the absence of CuO, it occurs at 1340 and 1290 °C using the co-impregnation and sequential processes, respectively. In addition, the materials with a CuO:Nb_2O_5 ratio of 1:1 and copper oxide content >2 wt% did not present that transition phase. This indicates a strong influence of CuO over Nb_2O_5 crystallites. XRD studies confirmed this interaction, showing the patterns of Cu and Nb oxides (for most of the samples prepared by both methods) and the presence of a third component (copper niobium oxide) on the samples with CuO content $\geqslant 10$ wt% when calcined at 800 °C for 6 h. FTIR, DRIFTS, and FT-Raman studies provided additional evidence of that interaction, which occurs not only on the surface hydroxyl groups of silica-alumina, but also on the surface hydroxyl groups of niobium pentoxide. The application of $CuO/Nb_2O_5/SiO_2$-Al_2O_3 materials in the oxidation of diesel soot particulates is promising; mixtures of the catalyst with a model particulate (Printex® U) lowered the oxidation temperature from 622 to 518 °C.

Keywords: Copper oxide; Niobium pentoxide; Silica-alumina; Diesel soot oxidation

1. Introduction

Materials containing metal oxide supports have been studied largely because of the various interactions among the different phases as well as their wide applications, including catalysis [1,2]. Niobium pentoxide is one of the most widely studied oxides. Despite its hydrophilic properties, the catalyst keeps its high acidity on the surface, exhibiting enhanced activity, selectivity, and stability over many other solid acids. This water-tolerant behavior makes this catalyst an interesting alternative for reactions in which water is involved [3]. Several roles and applications of niobium in catalysis have been detailed recently [4,5].

Supporting small amounts of oxides on high-specific surface area matrices produces new surface species with structural features that control the activity and selectivity of these new materials. The combination of two or more metal oxides on the surface produces a complex system with multiple functions of each oxide and often leads to new properties. As a result, these studies have become an important research area in catalysis [6–8].

Supported Nb_2O_5 on silica-alumina has been characterized recently, and preliminary catalytic activity has been observed in esterification reactions [9]. The supported material showed greater thermal stabilization of niobium pentoxide than the pure oxide. Supported niobium pentoxide crystallizes, forming a mixture of only orthorhombic and monoclinic phases with thermal treatments at 800 °C; in comparison, pure Nb_2O_5 forms the first crystalline phase (hexagonal, TT) at 450 °C. At Nb_2O_5 concentrations of 2–5 wt%, isolated species may predominate, whereas at about 10–15 wt%, a two-dimensional overlayer is formed on the SiO_2-Al_2O_3 surface [9]. Accordingly, different

---

* Corresponding authors. Fax: +55 61 3368 6901.
E-mail addresses: jdias@unb.br (J.A. Dias), scdias@unb.br (S.C.L. Dias).

0021-9517/$ – see front matter © 2007 Elsevier Inc. All rights reserved.
doi:10.1016/j.jcat.2006.12.022

catalytic sites are anticipated to have distinct activities from the bulk phases of the isolated oxides.

Copper oxide has been supported on different matrices with applications in many areas involving environmental catalysis [10,11], particularly for abatement of nitrogen oxide species (e.g., NO, NO_2, and N_2O) or production of hydrogen from alcohols. The presence of the CuO phase is very important in the activity of the various catalysts proposed for these processes [12]. Extensive studies of CuO supported on silica-alumina have been reported [12–16]. The dispersion of CuO on different supports depends on the copper content, nature of the support, deposition method, and interaction of copper precursor with the acidic sites of the support. Using the adsorption method starting from $Cu(H_3CCOO)_2$, a monolayer was reached with about 7–9 wt% of Cu on a commercial silica-alumina support (Grace). Also, XRD of samples containing 0.2–12 wt% of Cu (prepared by chemisorption–hydrolysis method using $Cu(NO_3)_2$ as a precursor) showed no bulk CuO phase for calcination at 350 °C [16]. It has been concluded that highly dispersed isolated copper ions predominate on silica-alumina surfaces for lower contents of CuO [13–15].

Particulate matter (PM), nitrogen and sulfur oxides, and unburned hydrocarbons are among the main pollutants in diesel engine emissions [17]. PM comprises fine solid or liquid particles (100 nm < diameter < 10 nm) suspended in gas. Although PM is naturally present in the atmosphere, its production by combustion of fossil fuels is responsible for the greatest portion released into the air [18]. As a result, emission control is of prime importance. Legislation concerning PM emissions has steadily lowered the allowable limits [19,20]. Because of the hazardous nature of diesel soot, the literature addresses many issues concerning the problem and progress in the development of devices to decrease PM emissions from engines. The solutions proposed to meet the standards frequently involve catalytic oxidation reactions carried out in particulate filters [17,18]. The literature indicates that the most active oxides in the soot combustion contain metals, which are capable of performing redox cycles during the combustion process [21]. The most frequently cited oxides are V_2O_5, CuO, MoO_3, MnO_2, Fe_2O_3, WO_3, La_2O_3, and CeO_2 [22,23]. Moreover, the addition of different promoters (e.g., K, Cs) has enhanced the activity of the most promising catalysts, as reported in the literature [24–26]. The presence of CuO and Nb_2O_5 in some prepared materials makes them potential candidates for the soot oxidation reaction.

This work deals with the preparation of the combined oxides, CuO and Nb_2O_5, over silica-alumina support. The influence of CuO on the properties of supported niobium pentoxide was evaluated. The catalytic activity of the most promising materials was verified in diesel soot particulate oxidation. For the structural characterization, X-ray powder diffraction (XRD), Fourier transform infrared spectroscopy (FTIR), diffuse reflectance infrared Fourier transform spectroscopy (DRIFTS), Raman with Fourier transform (FT-Raman), and thermal analysis (TG and DTA) were used.

2. Experimental

2.1. Preparation of $CuO/Nb_2O_5/SiO_2$-Al_2O_3 materials

Two methods were used for preparing the catalysts. In series A, the precursors were added simultaneously (co-impregnation). Aqueous solutions of $Cu(NO_3)\cdot 3H_2O$ (VETEC, Brazil) and $NH_4[NbO(C_2O_4)_2(H_2O)_2]\cdot(H_2O)_n$ (Companhia Brasileira de Mineração e Metalurgia, Brazil) were added to activated silica-alumina [9] (Aldrich, 12 wt% Al_2O_3, 475 $m^2\,g^{-1}$, 0.77 $cm^3\,g^{-1}$) to obtain a 1:10 ratio (mass to volume) of solids to water. The amount of copper and niobium oxides varied from 0.5 to 25 wt% CuO and from 5 to 25 wt% Nb_2O_5. Each slurry sample was stirred at 80 °C until all of the water evaporated. Then the solid was removed, ground to finer particles, placed in a vacuum oven at 100 °C, and stored for further calcination treatment.

In series B, the niobium precursor was impregnated (under the same experimental conditions described above) and the resulting solid was calcined at 600 °C for 3 h. Then copper was impregnated, followed by evaporation of water at 80 °C. Finally, the resulting solid was dried at 100 °C in a vacuum oven and stored for further calcination. The amounts of copper and niobium oxides were varied from 0.5 to 2.5 wt% CuO and from 5 to 25 wt% Nb_2O_5. Table 1 shows the nominal composition of each prepared solid; elemental analysis by ICP-AES did not present any significant difference, as observed previously [9]. Niobic acid, $Nb_2O_5\cdot nH_2O$ (HY® 340), was supplied from CBMM. All other reagents used in this study were analytical grade and used as supplied.

2.2. XRD, spectroscopic and thermal techniques

Powder XRD was performed with a Rigaku D/Max-2A/C diffractometer using Cu$K\alpha$ radiation of 1.5418 Å (40 kV and 20 mA). A 2θ range from 2 to 90° was scanned at 1.8° min^{-1}.

Table 1
Nominal composition of various $CuO/Nb_2O_5/SiO_2$-Al_2O_3 solids

Sample[a]	Preparation method[b]	[CuO] (wt%)	[Nb_2O_5] (wt%)
0.5Cu5Nb94.5SiAl-A	A	0.5	5
1.0Cu10Nb89SiAl-A	A	1.0	10
1.5Cu15Nb80SiAl-A	A	1.5	15
2.5Cu25Nb72.5SiAl-A	A	2.5	25
2Cu2Nb96SiAl-A	A	2	2
5Cu5Nb90SiAl-A	A	5	5
10Cu10Nb80SiAl-A	A	10	10
15Cu15Nb70SiAl-A	A	15	15
25Cu25Nb50SiAl-A	A	25	25
0.5Cu0.5Nb98SiAl-B	B	0.5	5
1.0Cu10Nb89SiAl-B	B	1.0	10
1.5Cu15Nb80SiAl-B	B	1.5	15
2.5Cu25Nb72.5SiAl-B	B	2.5	25

[a] The figures in the formula refer to the mass percentage of the respective oxides (CuO, Nb_2O_5, and SiO_2-Al_2O_3).

[b] Preparation by co-impregnation (A) and sequential impregnation of precursor solutions (B).

The crystalline and phase assignments were performed comparing the PDF files from International Centre for Diffraction Data (ICDD) included in the database of the JADE 3.0 software for XRD analysis.

FT-Raman, FTIR, and DRIFTS spectra were acquired on a Bruker Equinox 55 spectrometer equipped with a DTGS detector. FTIR and DRIFTS spectra were obtained with 256 scans and a resolution of 4 cm^{-1}. The samples were calcined before the measurements, and the spectra were acquired at ambient conditions, except for DRIFTS. Raman spectra were obtained with 1024 scans and resolution of 2 cm^{-1} in the hydrated samples packed into sample cups. The Raman laser excitation (Nd:YAG) wavelength and power were 1064 nm and 126 mW, respectively, with the signal detected by a liquid nitrogen-cooled Ge detector in a Bruker FRA 106/S module. The spectra were baseline-corrected and smoothed using polynomial functions. Infrared absorption curves were recorded in 1 wt% pellets prepared with dried KBr. DRIFTS spectra were registered within a Harrick diffuse reflectance accessory (Praying Mantis™), equipped with a high-temperature chamber and KBr windows. Before acquisition, each sample was heated to 300 °C under dry nitrogen flow for 30 min and then cooled. The spectra were acquired as reflectance against an alignment mirror and converted to Kubelka–Munk units after baseline correction.

TG and DTA data were obtained in a simultaneous TG-DSC (TA Instruments model SDT 2960), with a scan rate of 10 °C min^{-1}, from room temperature up to 1400 °C under a nitrogen (99.999%) flow of 110 mL min^{-1}.

2.3. Thermal activation of the catalysts

After preparation and before many of the experimental measurements, the samples were calcined in a muffle furnace (EDG model EDG3PS) under static air conditions in porcelain crucibles, at a heating rate of 14 °C min^{-1}. The temperature was either 300 or 800 °C. Other calcination temperatures are indicated on the respective experiment.

2.4. Catalytic tests for diesel soot oxidation

The catalyst activities were evaluated in the oxidation reaction of standard soot produced in a fuel burner (Printex® U; Degussa). The Printex® U was mixed with the catalyst at a mass ratio of 1:10. The mixing process was carried out in an agate mortar to promote tight contact between the components. The mixture (∼15 mg) was submitted to a temperature ramp from room temperature (∼25 °C) to 800 °C, using air (99.999% with 110 mL min^{-1} flow) at a rate of 10 °C min^{-1}. The curve (TG-DTA) was recorded using a simultaneous TG-DSC (SDT 2960).

3. Results and discussion

3.1. Analyses of the precursor decomposition

The structural transformations of niobium pentoxide are highly dependent on temperature, heating time, and the type of support in which the oxide is dispersed [27]. Silica-alumina did not present any crystalline powder diffraction pattern in the temperature range studied. It has been reported that when supported on silica-alumina, Nb_2O_5 reaches a crystalline form (mixture of phases T, M, and H) only after heating at or above 800 °C, in contrast to pure Nb_2O_5, which starts to crystallize at about 450 °C (hexagonal phase, TT) [9]. Because this system has two supported oxides, the thermal decomposition of the precursors was initially examined (Fig. 1). Niobium oxalate gradually decomposes to niobium pentoxide under heating treatment. Pure crystalline oxalate revealed a halo-amorphous pattern at heating temperatures of about 300–400 °C for 6 h, similar to the pattern observed for $Nb_2O_5/SiO_2\text{-}Al_2O_3$ heated at 300 °C for 6 h. The oxalate calcined at 700 °C for 3 h showed a pattern similar to the niobium pentoxide treated at 800 °C for 6 h, which exhibited a predominantly orthorhombic phase. On the other hand, copper nitrate degrades, forming copper oxide at about 300 °C, typically exhibiting the most intense reflections at $2\theta = 35.5$ and 38.7° (PDF 05-0661). Copper oxide and niobium pentoxide supported on silica-alumina (10 wt% CuO and 10 wt% Nb_2O_5) calcined at 300 °C for 6 h displayed only the two reflections relative to CuO, demonstrating that this is the sole crystalline phase under these treatment conditions.

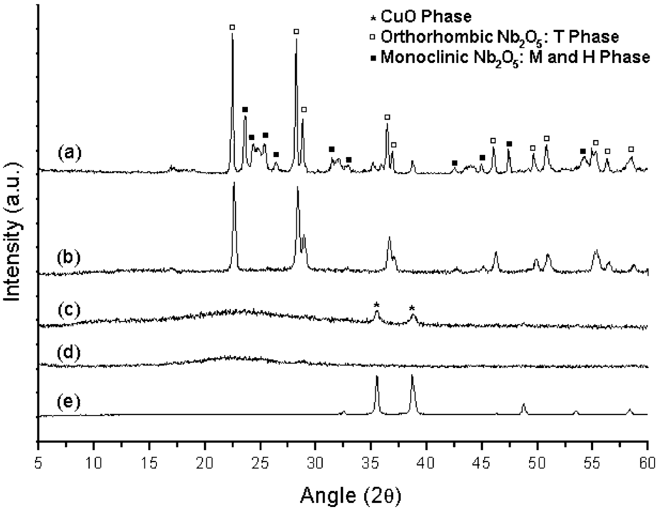

Fig. 1. XRD patterns at different calcination conditions for: Nb_2O_5 at 800 °C/6 h (a); $NH_4[NbO(C_2O_4)_2(H_2O)_2]\cdot(H_2O)_n$ at 700 °C/3 h (b); 10% CuO/10% $Nb_2O_5/SiO_2\text{-}Al_2O_3$ at 300 °C/6 h, series A (c); 10% $Nb_2O_5/SiO_2\text{-}Al_2O_3$ at 300 °C/6 h (d); $Cu(NO_3)\cdot 3H_2O$ at 300 °C/6 h (e).

Thermal degradation of the $CuO/Nb_2O_5/SiO_2\text{-}Al_2O_3$ system was also followed by FTIR (Fig. 2). Niobium oxalate and copper nitrate precursors exhibited absorption bands at about 1718, 1689, 1450, 1400, 1298, and 950 cm^{-1}. The bands at 1450, 1298, and 950 cm^{-1} can be attributed to stretching vibrations of N–O bonds in the Cu precursor [28]. The absorptions at 1718, 1689, and 1400 cm^{-1} are assigned to two stretching vibration modes of C=O, a stretching combination of ν(C–O) and ν(C–C), and ν(N–H), respectively, associated with the niobium precursor. Decreasing intensity of these absorption bands after treatment at 100 °C for 2 h and a complete disappearance after treatment at 300 °C for 6 h was observed.

3.2. Support coverage analysis

To gain more information about the coverage behavior of the complex mixed oxide system, the isolated supported oxides were evaluated. The copper oxide supported on silica-alumina system was prepared by impregnation of copper nitrate with 2, 5, 10, 15, and 25 wt% in a similar procedure as described for the mixed-oxide catalysts. The prepared samples were calcined at 300 and 800 °C, and the XRD patterns were obtained (Figs. 3 and 4). After calcination at 300 °C, the CuO/SiO_2-Al_2O_3 catalysts showed a typical crystalline CuO phase ($2\theta = 35.5$ and 38.7°) for >10 wt% of copper oxide. In contrast, for calcination at 800 °C, the samples with CuO loadings as low as 10 wt% exhibited a crystalline phase. An additional peak was assigned to SiO_2 in the quartz form ($2\theta = 26.6°$) for the material calcined at 800 °C.

Detailed studies have shown that copper oxide species are well dispersed in many different types of supports, depending on the amount of copper and the method of preparation [13]. Calcination at 350 °C for 4 h did not reveal any detectable crystalline phase up to 12 wt% of CuO, in agreement with scanning electron microscopy (SEM) results [16].

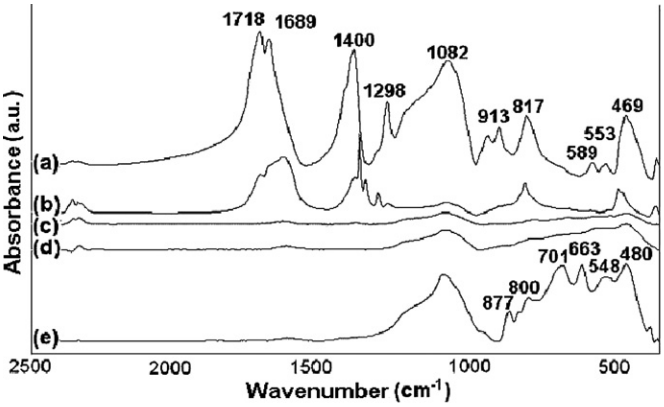

Fig. 2. FTIR spectra of 25% CuO/25% Nb_2O_5/SiO_2-Al_2O_3 without calcination (a) and calcined at: 100 °C/2 h (b); 300 °C/2 h (c); 500 °C/6 h (d); 800 °C/2 h (e).

The theoretical monolayer of CuO over silica-alumina (475 $m^2\,g^{-1}$) is about 48 wt%, calculated by considering the face dimension (direction a–c) of the crystalline unit cell for CuO placed on silica-alumina surface [29,30]. Based on the XRD results, it may be inferred that samples calcined at 300 °C for 6 h with CuO loadings of about 10–15 wt% correspond to the monolayer coverage. At CuO loading $\geqslant$10 wt%, calcination at 800 °C for 6 h produced distinct peaks related to crystalline CuO. A qualitative indication for estimating the species at monolayer coverage is by sample color [16,31]. The prepared samples with 2 and 5 wt% are pale blue, the 10 wt% solid is blue-greenish, and the 15 and 25 wt% solids are green. This behavior has been interpreted as indicative of isolated Cu^{2+} species (at lower CuO content, e.g., 2 and 5 wt%) and oxo-cation of $[Cu–O–Cu]^{2+}$ (at higher CuO content, e.g., 15 and 25 wt%) [16,31]. Thus, the pale-blue and green sample colors are indicative of sub-monolayer and above-monolayer coverage.

The Nb_2O_5/SiO_2-Al_2O_3 system, which has been studied in detail elsewhere [9], also should be considered. The theoretical monolayer for this material is about 39.6 wt% niobium pentoxide loading, calculated based on the dimension of 0.32 nm^2 per Nb_2O_5 crystal unit reported in the literature [32]. However, the experimental data based on XRD and Raman measurements have established that the actual monolayer is 10–15 wt% Nb_2O_5 loading [9]. Thus, the materials with 2 and 5 wt% are below the monolayers, and those with 15–25 wt% are above monolayer. It should be mentioned that all of these solids are off-white when calcined at 800 °C for 6 h and exhibit an amorphous XRD pattern when calcined at 300 °C for 6 h. Before examining the crystalline properties of the CuO/Nb_2O_5/SiO_2-Al_2O_3 catalysts, we present thermal analysis results to provide insight into the effects of the preparation methods.

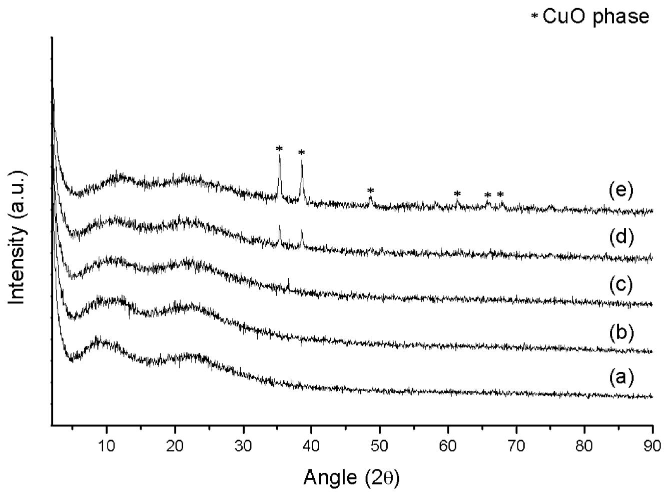

Fig. 3. XRD of CuO/SiO_2-Al_2O_3 calcined at 300 °C/6 h with: 2% (a); 5% (b); 10% (c); 15% (d); and 25 wt% (e) of CuO, respectively.

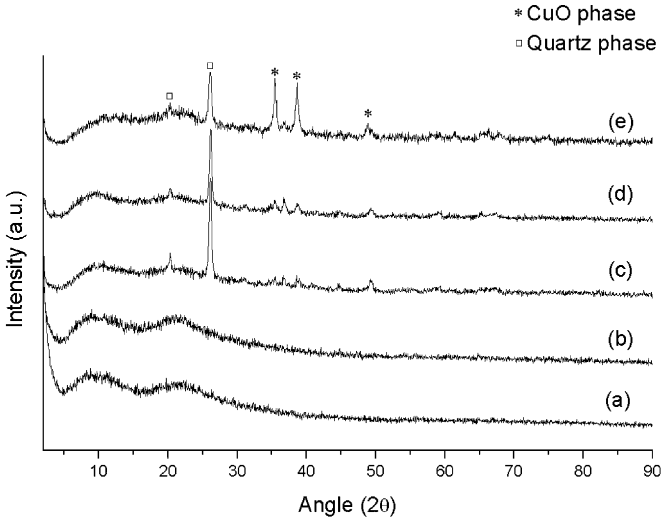

Fig. 4. XRD of CuO/SiO_2-Al_2O_3 calcined at 800 °C/6 h with: 2% (a); 5% (b); 10% (c); 15% (d); and 25 wt% (e) of CuO, respectively.

3.3. Thermal analysis of $CuO/Nb_2O_5/SiO_2$-Al_2O_3 catalysts

The DTA curves (Figs. 5A–5C) demonstrate important differences in the preparation procedures. As pointed out previously [9], hydrated niobium pentoxide shows a phase transition at 568 °C (phase T), whereas silica-alumina displays no evidence of a crystalline phase under these experimental conditions. Conversely, the samples with Cu and Nb precursors exhibit some differences from the system containing only Nb. Nb_2O_5/SiO_2-Al_2O_3 exhibits a phase transition at about 1356 °C, which probably can be assigned to the formation of phase H. Preparation involving co-impregnation (series A) with a CuO:Nb_2O_5 ratio of 1:10 shows a transition phase at about 1340 °C (Fig. 5A). This exothermic peak decreased in area as the amount of CuO increased up to 1.5 wt% and practically disappeared at a CuO content of 2.5 wt% (Fig. 5A, d). This is demonstrated by the DTA curves (Fig. 5B) of the samples with a CuO:Nb_2O_5 ratio of 1:1 prepared by the same method (series A), which show no phase transition. It should be noted that Fig. 5B was obtained under air atmosphere with the samples dried under vacuum at 100 °C. The thermal oxidative decomposition of the precursors was evident at about 300 °C, with an initial water release at about 90 °C. This decomposition was also observed under nitrogen flow, but as an endothermic event in this case (not shown). Thus, it may be concluded that increasing CuO content inhibits the transition phase of Nb_2O_5.

The DTA curves (Fig. 5C) for the samples prepared by sequential impregnation (series B) with a CuO:Nb_2O_5 ratio of 1:10 show that precalcination at 600 °C for 3 h totally decomposed the niobium precursor. The degradation of the small amount of copper nitrate occurred at about 300 °C, although this is evident only in the DTG curve (not shown). The endothermic peak at 90 °C is related to physisorbed and chemisorbed water. The exothermic peak related to the transition phase of Nb_2O_5 occurred at lower temperatures ($\sim$1290 °C) and was observed mainly for the samples with lower CuO contents (0.5 and 1.0 wt%). These results demonstrate the significant effect of CuO on the supported Nb_2O_5. Thus, the co-impregnation method (series A) produced materials with higher thermal stability than the sequential impregnation method (series B).

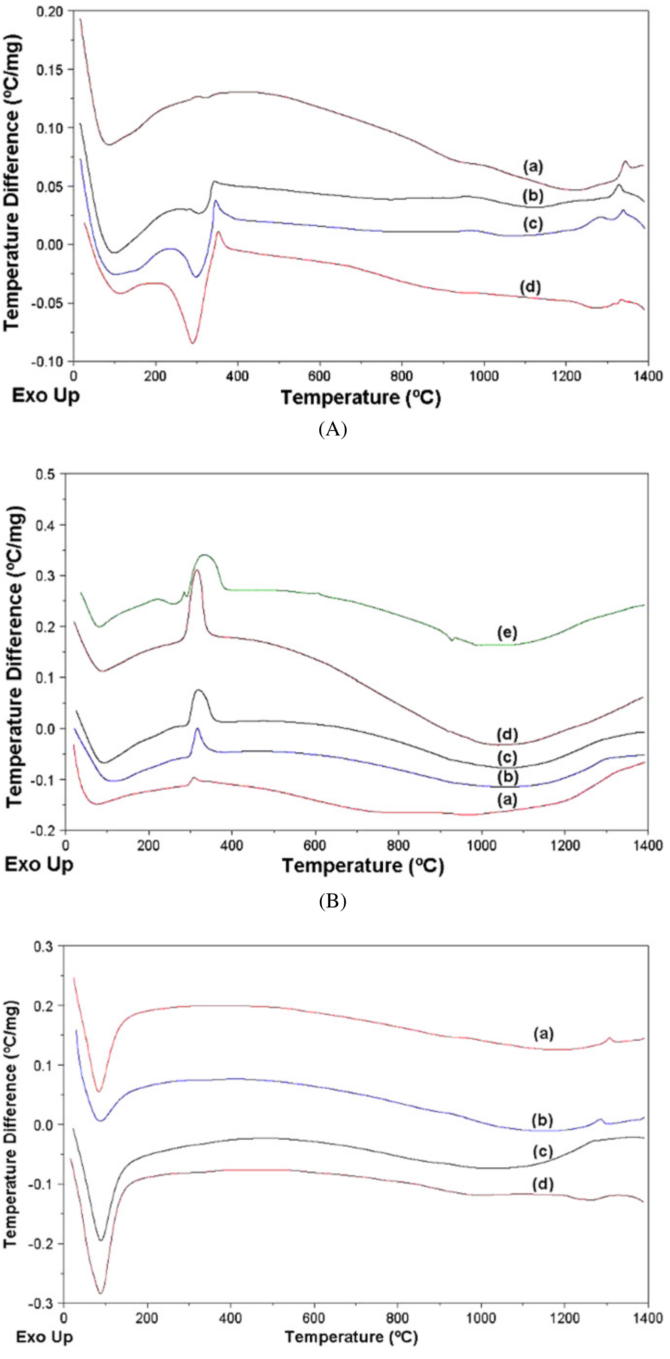

(A)

(B)

(C)

Fig. 5. (A) DTA curves for $CuO/Nb_2O_5/SiO_2$-Al_2O_3 prepared by co-impregnation (series A) with a ratio of 1:10 CuO:Nb_2O_5; 0.5% (a); 1% (b); 1.5% (c); 2.5 wt% of CuO (d), respectively. (B) DTA curves for $CuO/Nb_2O_5/SiO_2$-Al_2O_3 prepared by co-impregnation (series A) with a ratio of 1:1 CuO:Nb_2O_5; 2% (a); 5% (b); 10% (c); 15% (d); 25 wt% of CuO (e), respectively. Note that these curves were obtained under air (110 mL min^{-1}). (C) DTA curves for $CuO/Nb_2O_5/SiO_2$-Al_2O_3 prepared by sequential impregnation (series B) with a ratio of 1:10 CuO:Nb_2O_5; 0.5% (a); 1% (b); 1.5% (c); 2.5 wt% of CuO (d), respectively.

3.4. XRD of $CuO/Nb_2O_5/SiO_2$-Al_2O_3

Based on the thermal stability results, further detailed studies of the catalysts prepared by co-impregnation (series A) were developed. Fig. 6 shows the XRD of the $CuO/Nb_2O_5/SiO_2$-Al_2O_3 materials prepared by co-impregnation (method A) and calcined at 800 °C for 6 h. The samples with a CuO:Nb_2O_5 ratio of 1:10 and with 0.5 and 1.0 wt% CuO exhibited an amorphous pattern (Figs. 6a–6b). In contrast, the sample with 1.5 wt% displayed peaks at $2\theta \cong 23.3$, 24.5, and 28.3, which are typical of the monoclinic phase (M and H) of niobium pentoxide (Fig. 6c). In contrast, the materials prepared with a CuO:Nb_2O_5 ratio of 1:1 (Figs. 6d–6g) exhibited different characteristics. No crystalline pattern can be detected in samples with lower CuO contents (2 and 5 wt%), but different phases can be seen for those with higher CuO contents (10 and 15 wt%). Nb_2O_5 ($2\theta \cong 24.3$, 25.1) and CuO ($2\theta \cong 35.5$; 38.7) can be seen, along with two new reflections at $2\theta \cong 29.9$ and 30.5 not found in the patterns of the former oxides.

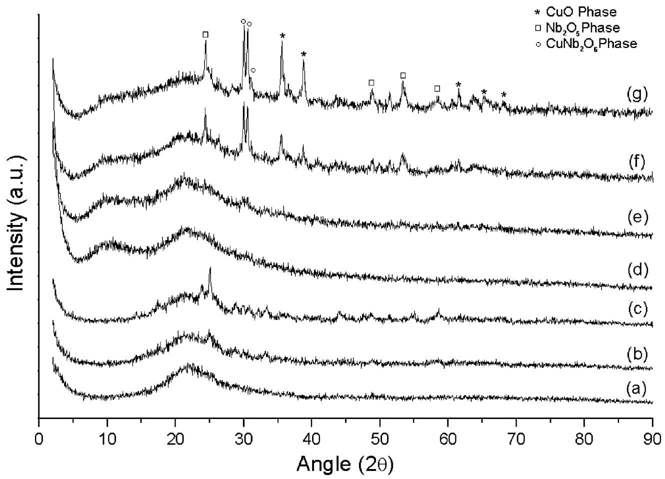

Fig. 6. XRD of $CuO/Nb_2O_5/SiO_2$-Al_2O_3 (series A) prepared with a 1:10 ratio of CuO:Nb_2O_5; 0.5% (a); 1% (b); 1.5% (c); and prepared with 1:1 ratio: 2% (d); 5% (e); 10% (f); 15 wt% of CuO (g), respectively. All samples were calcined at 800 °C/6 h.

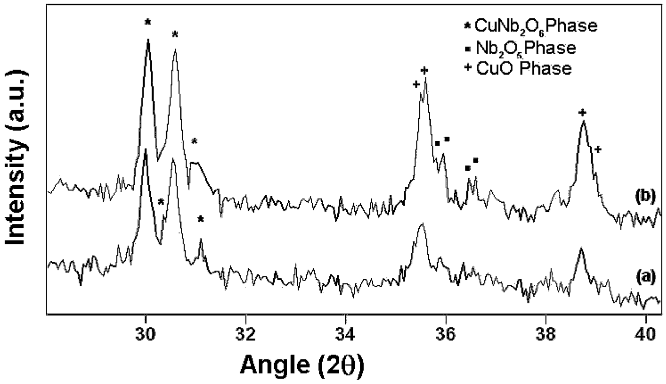

Fig. 7. Expanded XRD of $CuO/Nb_2O_5/SiO_2$-Al_2O_3 (series A) prepared with a 1:1 ratio of CuO:Nb_2O_5 with 10% (a) and 15 wt% of CuO (b), respectively. All samples were calcined at 800 °C/6 h.

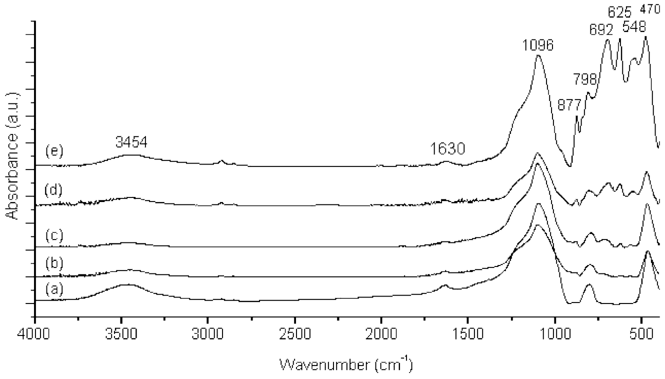

Fig. 8. FTIR spectra of $CuO/Nb_2O_5/SiO_2$-Al_2O_3 (series A) prepared with a 1:1 ratio of CuO:Nb_2O_5; 2% (a); 5% (b); 10% (c); 15% (d); 25 wt% of CuO (e), respectively. All samples were calcined at 800 °C/6 h.

To examine these reflections in detail, an expanded XRD curve ($20° < 2\theta < 40°$) was plotted (Fig. 7). The peaks were assigned to the respective Nb_2O_5 and CuO oxide phases. Those two new reflections confirmed the presence of copper niobium oxide ($CuNb_2O_6$), according to the PDF 45-0561. At lower calcination temperatures (300 °C for 6 h) and lower CuO content (0.5–5 wt%), no peaks were recorded in the XRD, confirming a halo-amorphous pattern. However, for CuO content $\geqslant$10 wt%, only peaks at $2\theta = 35.5$ and 38.7 were present, characteristic of crystalline CuO, and no reflections from Nb_2O_5 or $CuNb_2O_6$ were observed (not shown). This finding was expected, because bulk Nb_2O_5 is amorphous under these conditions and the temperature is not high enough for $CuNb_2O_6$ formation. It can be concluded that increasing the amount of copper oxide over 10 wt% favored the formation of a mixed-oxide phase between Cu and Nb at higher calcination temperatures (800 °C for 6 h), whereas at lower temperatures (300 °C for 6 h), the only crystalline phase observed was at CuO content >5 wt%.

Considering the experimental results of the isolated supported oxides and the samples of $CuO/Nb_2O_5/SiO_2$-Al_2O_3 obtained by co-precipitation, it can be inferred that the monolayer for these materials is 5–10 wt% of both supported oxides. Another qualitative indication is provided by the color of the samples. The samples with 0.5–5 wt% CuO are white-grayish, whereas those with 10–25 wt% CuO are gray-blackish. Because CuO is a black solid, the material turns blacker as the crystalline copper oxide content increases. This finding is supported by the fact that XRD revealed no CuO phase in materials with a CuO:Nb_2O_5 ratio of 1:10 (i.e., CuO content of 0.5–2.5 wt%) calcined at either 300 or 800 °C.

Based on these results, and mainly on the thermal analysis, co-impregnation is considered the most promising method, producing materials with higher thermal stability for the transition phase of niobium pentoxide. In addition, the samples with a CuO:Nb_2O_5 ratio of 1:1 exhibit the best behavior, because they present no phase transformation at temperatures up to 1400 °C and provide the possibility of controlling the species generated on the silica-alumina surface by calcination either at lower temperatures (300 °C for 6 h) or higher temperatures (800 °C for 6 h). Thus, the samples with a CuO:Nb_2O_5 ratio of 1:1 were further characterized by FTIR, DRIFTS, and Raman spectroscopy.

3.5. FTIR, DRIFTS, and Raman spectroscopy of $CuO/Nb_2O_5/SiO_2$-Al_2O_3

The FTIR spectra for the samples prepared by co-impregnation and calcined at 800 °C for 6 h are shown in Fig. 8. As observed earlier for the Nb_2O_5/SiO_2-Al_2O_3 system [9], the main peaks of silica-alumina were predominantly ν_{as}(Si–O) $\sim$ 1100 cm^{-1} with a shoulder at $\sim$1200 cm^{-1}, external ν(Si–O^{-}) $\sim$ 930 cm^{-1}, ν_s(Si–O) $\sim$ 805 cm^{-1}, external δ(Si–O^{-}) $\sim$ 576 cm^{-1}, and δ(Si–O–Si) $\sim$ 467 cm^{-1}, along with water (at 3454 and 1602 cm^{-1}). A closer look reveals important characteristics of the supported oxides. The band at 576 cm^{-1} shifted to 548 cm^{-1}, indicating that Nb and Cu react with Si–OH groups to form new surface species. This band shift is associated with substitution of the stronger O–H bonding for Si–O–Nb or Si–O–Cu, weakening the Si–O bond. Other absorptions related to Nb–O bonding were also observed due to the presence of Nb_2O_5. The original wavenumbers of these Nb–O bondings, 666 and 620 cm^{-1}, were shifted to 692 and 625 cm^{-1}.

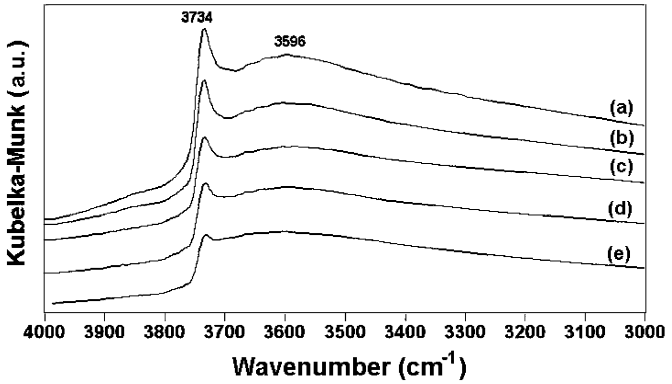

Fig. 9. DRIFTS spectra of $CuO/Nb_2O_5/SiO_2$-Al_2O_3 (series A) prepared with a 1:1 ratio of CuO:Nb_2O_5; 2% (a); 5% (b); 10% (c); 15% (d); 25 wt% of CuO (e), respectively. All samples were calcined at 800 °C/6 h.

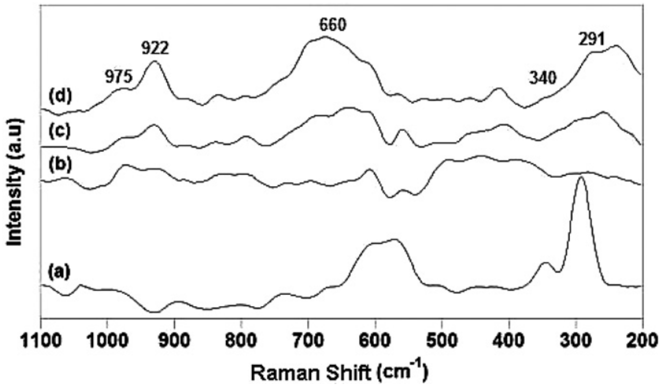

Fig. 10. Raman spectra of $CuO/Nb_2O_5/SiO_2$-Al_2O_3 (series A) prepared with a 1:10 ratio of CuO:Nb_2O_5; pure CuO (a); 0.5% (b); 1.0% (c); 1.5 wt% of CuO (d), respectively. All samples were calcined at 800 °C/6 h, except CuO (300 °C/6 h).

These data point toward interaction of copper with niobium, forming species such as Nb–O–Cu on the silica-alumina surface. Because of the lower electronegativity of Cu compared with Nb, the shift is directed to higher wavenumbers by the formation of stronger Nb–O bonding. The main vibrations of CuO (at 476, 537, and 588 cm^{-1}) [33] are not evident in the studied spectra, even though their influence on the energy of the closest bands of the materials cannot be discharged. Consequently, the interaction of Cu and Nb species on the silica-alumina surface probably occurs through the formation of Si–O–Nb, Si–O–Cu, and Nb–O–Cu bonds.

To confirm the precursor reactions on the support surface, DRIFTS spectra of the samples calcined at 800 °C for 6 h were obtained in the OH vibration region. It was previously shown that niobium pentoxide reacts increasingly and in a selective manner through hydroxyl functionality on the silica-alumina surface [9]. Pure CuO calcined at 300 °C displayed a wide band with no evidence of a specific surface hydroxyl. Niobium pentoxide showed a spectrum that is highly dependent on the calcination conditions. Under calcination at 800 °C for 6 h, the strongest absorption occurred at 3430 cm^{-1}, with a smaller wide band at 3670 cm^{-1}. Silica-alumina presented an intense peak at 3740 cm^{-1} (isolated silanols) and a broad band centered at 3596 cm^{-1} (hydrogen-bonded silanol). The spectra of $CuO/Nb_2O_5/SiO_2$-Al_2O_3 (Fig. 9) show a pattern similar to that previously observed for Nb_2O_5/SiO_2-Al_2O_3 [9]. The isolated hydroxyls (3740 cm^{-1}) from silica-alumina surface are the first sites that react with Cu and Nb precursors, and they are consumed as the concentration of metal increases. However, compared with the same niobium content level in the Nb_2O_5/SiO_2-Al_2O_3 catalyst (sample with 25 wt% of Nb_2O_5), the silanols were not completely neutralized in the presence of copper oxide. This result, coupled with the displacement of the Nb–O–Nb bands in the IR spectra, confirms that at least part of the copper oxide was connected to the niobium species and not directly to the support. Even though some water was adsorbed on the silica-alumina surface (represented by the broad band at 3596 cm^{-1}), this band decreased in intensity as the amount of the precursors increased. Finally, considering the formation of copper niobate (detected by XRD) and the data obtained by FTIR and DRIFTS, there is sufficient evidence of the strong interaction between Cu and Nb on the silica-alumina surface.

Raman spectroscopy can reveal additional information about the direct interaction between Cu and Nb. The spectra of the catalysts without copper (Nb_2O_5/SiO_2-Al_2O_3) calcined at 800 °C for 6 h obtained under hydrated conditions showed very broad bands for the samples with 2, 5, and 10 wt% Nb_2O_5, characteristic of the presence of isolated and/or bidimensional niobium species [9]. On the other hand, the samples with 15, 20, and 25 wt% displayed absorptions assigned to the presence of different bulk phases of niobium pentoxide, such as orthorhombic (T) and monoclinic (M, H) phases [9].

Raman spectra of the hydrated catalysts containing 2, 5, 10, 15, and 25 wt% of supported CuO on silica-alumina were obtained at 300 and 800 °C for 6 h. The results indicated only a very weak signal of bulk CuO ($\sim$295 cm^{-1}) for the samples with 15–25 wt% CuO calcined at 300 °C for 6 h (results not shown). No bands could be detected for the samples calcined at 800 °C for 6 h. This may indicate some limitations of the experimental apparatus used in this investigation, because the absorption intensity of CuO is not as strong and is quite within the limit of the signal produced by silica-alumina support. Similar effects were observed for CuO supported on ceria using the same kind of spectrometer [34].

On the other hand, Raman spectra of the samples with a CuO:Nb_2O_5 ratio of 1:10 calcined at 800 °C for 6 h and obtained under hydrated conditions (Fig. 10) showed bands that can be attributed mainly to different niobium pentoxide vibrations. Considering that crystalline CuO showed band vibrations at 295 (most intense), 350, and 636 cm^{-1} [35], and these were not detected in the CuO/SiO_2-Al_2O_3 calcined at 800 °C for 6 h, no large contribution from CuO can be expected on the spectra of $CuO/Nb_2O_5/SiO_2$-Al_2O_3 catalysts, even for the broad band between 500 and 700 cm^{-1} (Fig. 10a). The bands are assigned based on similarities of the earlier study of Nb_2O_5/SiO_2-Al_2O_3 catalysts [9]. The hydrated spectra of the catalyst material with 0.5 wt% CuO and 5 wt% Nb_2O_5 were very similar to those of the 5 wt% Nb_2O_5/SiO_2-Al_2O_3 mater-

Table 2
Possible species present on silica-alumina surface, according to CuO and Nb_2O_5 contents prepared by co-impregnation of precursor solutions

Catalyst composition[a]	Calcination (°C)	Type of species[b]
	$CuO/Nb_2O_5/SiO_2$-Al_2O_3 1:10 ratio	
0.5–1.0	300 or 800	I-CuO_x and/or Nb_2O_x and/or P-Nb_2O_x
1.5–2.5	300	I-CuO_x and A-Nb_2O_5
1.5–2.5	800	I-CuO_x and C-Nb_2O_5
	$CuO/Nb_2O_5/SiO_2$-Al_2O_3 1:1 ratio	
2–5	300 or 800	I-CuO_x and/or Nb_2O_x and/or P-Nb_2O_x
10–25	300	C-CuO and A-Nb_2O_5
10–25	800	C-CuO, C-Nb_2O_5, and C-$CuNb_2O_6$
	Nb_2O_5/SiO_2-Al_2O_3	
2–10	800	I-Nb_2O_x and/or P-Nb_2O_x
15–25	800	C-Nb_2O_5
	CuO/SiO_2-Al_2O_3	
2–10	300	I-CuO_x
15–25	300	C-CuO
2–5	800	I-CuO_x
10–25	800	C-CuO and C-SiO_2 (quartz)

[a] Catalyst contents are expressed in wt%.
[b] A—amorphous, C—crystalline, I—isolated, P—polymerized.

ial, that is, a very broad band indicating the presence of either isolated or bidimensional well-dispersed species on the surface, because no crystalline phase was detected by XRD. For the sample with 1 wt% CuO (10 wt% Nb_2O_5) broad bands were observed at ~975, ~922, and ~660 cm^{-1}. The shoulder at about 975 cm^{-1} has been attributed to the presence of isolated NbO_4 species on different supports (e.g., SiO_2, MCM-41) [36]. The band at ~922 cm^{-1} might be attributed to Nb=O present in a highly distorted octahedral species, although a possible contribution of SiO^- functionality cannot be ruled out, because DRIFTS results confirmed that not all hydroxyl groups were neutralized by the reaction with the precursors. The broad band centered at ~660 cm^{-1} has been attributed to Nb–O–Nb polyhedra (600–700 cm^{-1}) present in such species as NbO_6, NbO_7, and NbO_8 of the bulk pentoxide [9,37]. For the sample with 1.5 wt% CuO (15 wt% Nb_2O_5), the Raman spectra were similar to those of 1 wt% CuO, but the bands increased in intensities because of the higher niobium pentoxide content. Similar behavior was observed for the systems with Nb_2O_5/SiO_2-Al_2O_3 [9].

The influence of CuO on the surface species formed on the $CuO/Nb_2O_5/SiO_2$-Al_2O_3 catalysts are further demonstrated on the materials with a CuO:Nb_2O_5 ratio of 1:1. No Raman bands could be detected for the hydrated samples. This may be attributed to inhibition of Nb_2O_5 absorption through the interaction with CuO, because without CuO or with lower CuO contents, distinct bands were present in the spectra. Thus, all data obtained in this report point to the formation of distinct species on the silica-alumina surface according to the CuO and Nb_2O_5 contents and calcination temperatures. Based on the experimental results, the possible species for the catalysts of $CuO/Nb_2O_5/SiO_2$-Al_2O_3, Nb_2O_5/SiO_2-Al_2O_3, and CuO/SiO_2-Al_2O_3 are summarized in Table 2.

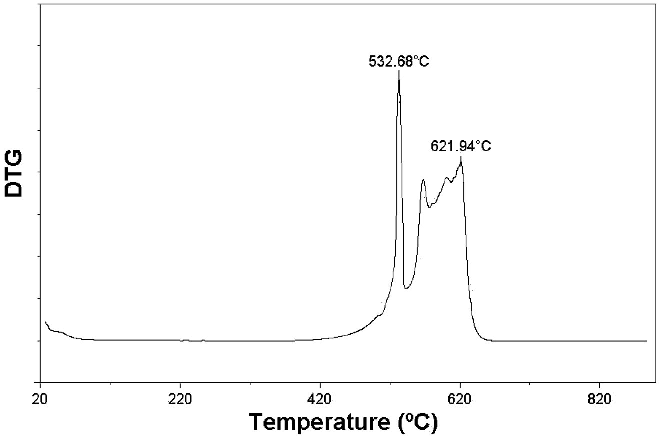

Fig. 11. DTG curve for Printex® U (reference material for diesel particulate oxidation) under air (110 mL min^{-1}) at a heating rate of 10 °C min^{-1}.

3.6. *Catalytic test for diesel soot oxidation*

The evaluation of catalytic activity was carried out in a model oxidation reaction of PM from diesel engines. It should be mentioned that the comparison of experimental results is not always straightforward, because of the differences in catalyst tests methodologies (e.g., model PM, ratio of soot to catalyst, conditions of gas flow, oxygen/air, and type of contact between catalyst and soot).

The activities were tested on the materials with a CuO:Nb_2O_5 ratio of 1:1, and the combustion process was simulated by studying the profile of the DTG curve obtained during the reaction of the catalyst mixed with diesel soot (Printex® U) under oxidative conditions. Comparing the temperature of the maximum mass loss, which is related to the oxidation process, allows evaluation of catalyst performance [38,39]. The mixture was prepared with the catalysts treated at either 300 or 800 °C for 6 h.

To evaluate the activity of the materials, we measured the activity of each oxide separately, along with the behavior of diesel soot. In all cases, a mixture of Printex® U with the material was done with a Printex® U:catalyst mass ratio of 1:10. Fig. 11 shows the DTG curve of the Printex® U, displaying distinct peaks at maximum temperatures of about 532, 566, 600, and 622 °C. These events are associated with the initial oxidation step of organic compounds adsorbed on the particulates (532 °C), their complete oxidation (566 and 600 °C), and oxidation of particulates (622 °C). The literature reports the standard temperature of oxidation for diesel soot as 600 °C [40]. Actually, this temperature depends on the exact chemical composition of the source soot, as well as on the method used to produce it. Because the highest rate for our Printex® U sample shows a mass loss at about 622 °C, we used this temperature to compare the performance of the tested materials.

The addition of the catalyst to Printex® U produces a variable decrease in the maximum temperature of the mass loss (T_{ox}), which is interpreted as the oxidation of the organic residues adsorbed on the soot, and of the PM itself. Fig. 12 shows the behavior of the mixtures and the effect of the temperature decrease. Note that silica-alumina showed no appre-

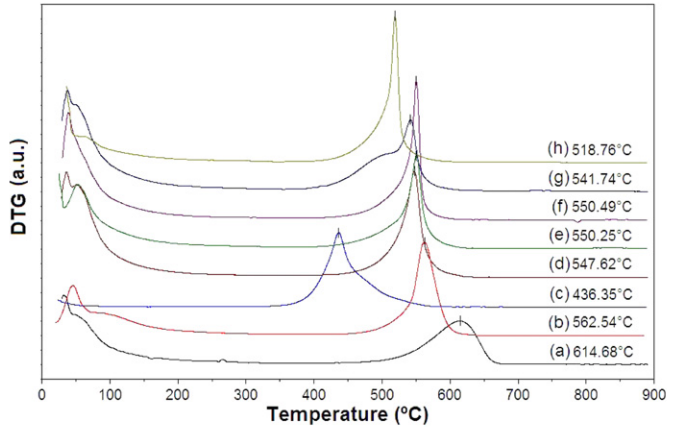

Fig. 12. DTG curves for the mixtures of 1:10 Printex® U:CuO/Nb_2O_5/SiO_2-Al_2O_3 (air at 110 mL min^{-1} and rate of 10 °C min^{-1}). The catalysts are: silica-alumina (a); Nb_2O_5 (b); CuO (c); 2% (d); 5% (e); 10% (f); 15% (g); 25 wt% of CuO (h) prepared by series A (1:1 ratio CuO:Nb_2O_5), respectively, and calcined at 300 °C/6 h. Maximum temperatures (T_{ox}) are listed for each catalyst.

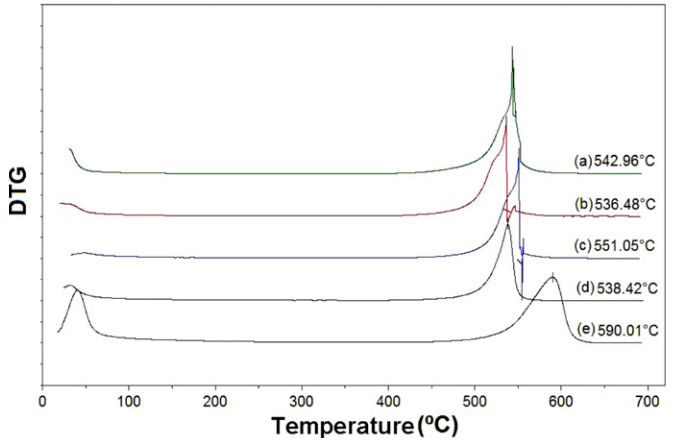

Fig. 13. DTG curves for the mixtures of 1:10 Printex® U:CuO/Nb_2O_5/SiO_2-Al_2O_3 (air at 110 mL min^{-1} and rate of 10 °C min^{-1}). The catalysts are: 2% (a); 5% (b); 10% (c); 15% (d); 25 wt% of CuO (e) prepared by series A (1:1 ratio CuO:Nb_2O_5), respectively, and calcined at 800 °C/6 h. Maximum temperatures (T_{ox}) are listed for each catalyst.

Table 3
Thermal characteristics of CuO/Nb_2O_5/SiO_2-Al_2O_3 calcined at 300 or 800 °C when mixed with Printex® U

Catalyst[a]	Onset (°C)	T_{ox} (°C)	Offset (°C)	O.R. (°C)[b]
2/300	519.06	547.45	566.53	47.47
5/300	527.12	550.43	569.47	42.35
10/300	519.37	550.17	563.35	43.98
15/300	433.62	541.32	562.24	128.62
25/300	458.34	518.76	539.81	81.47
2/800	536.33	590.01	611.07	74.74
5/800	523.11	560.7	571.54	48.43
10/800	512.84	551.05	554.27	41.43
15/800	501.08	536.48	541.05	39.97
25/800	507.97	542.96	557.19	49.22

The values are related to the onset, offset, maximum (T_{ox}) and range of oxidation (O.R.) for Printex® U.

[a] Catalyst loading (wt%)/calcination temperature (°C).

[b] O.R. = oxidation range.

ciable oxidation activity ($T_{ox} \sim 614$ °C). Pure Nb_2O_5 presented a small shift ($T_{ox} \sim 562$ °C) in the temperature oxidation of Printex® U, whereas pure CuO showed the greatest displacement ($T_{ox} \sim 436$ °C). Even though copper oxide is the most active, there have been no reports of systems using just this oxide, probably for technical and/or economic reasons. The literature reports that Nb_2O_5 is not active for graphite oxidation [41]. The CuO/Nb_2O_5/SiO_2-Al_2O_3 catalysts calcined at 300 °C for 6 h were tested in the oxidation of Printex® U and showed good activity (Fig. 12). The greater displacement at oxidation temperature occurred in the 25 wt% CuO catalyst ($T_{ox} \sim 518$ °C). The average mass loss for all samples was about 10 wt%, indicating no significant errors in the mixture preparation.

To verify the most active catalysts for the Printex® U oxidation, CuO/Nb_2O_5/SiO_2-Al_2O_3 solids calcined at 800 °C for 6 h were also tested under the same conditions (Fig. 13). A higher oxidation temperature (T_{ox}) was observed for all catalysts calcined at 800 °C, confirming the greater activity for the catalysts calcined at 300 °C. Moreover, a better comparison can be made not only with the T_{ox}, but also with other characteristics of the thermal profile, such as onset temperature and oxidation range. Table 3 shows that the temperature range in which the catalysts are active is wider for those calcined at 300 °C than for those calcined at 800 °C. Another interesting feature is that the 15 wt% CuO/Nb_2O_5/SiO_2-Al_2O_3 catalyst has the lowest onset temperature activation of the series (∼433 °C) and the highest temperature oxidation range (∼128 °C).

The isolated supported oxides (i.e., CuO/SiO_2-Al_2O_3 and Nb_2O_5/SiO_2-Al_2O_3 calcined at 300 °C) were also evaluated for soot oxidation (Fig. 14). It was observed that the presence of CuO leads to more active materials. The sample with 25 wt% CuO/SiO_2-Al_2O_3 lowered the soot oxidation temperature to ∼571 °C, and 25 wt% Nb_2O_5/SiO_2-Al_2O_3 showed no significant temperature shift ($T_{ox} \sim 618$ °C). These data confirm that the high activity of CuO/Nb_2O_5/SiO_2-Al_2O_3 is due to the copper species, and that the niobium species have a moderate promoting effect on the process. Actually, the results are promising because they were obtained in the absence of any traditional chemical promoters, such as alkaline metals [24–26]. The addition of various alkaline metal elements to the best catalysts is the subject of current investigations, results from which will be reported in the near future.

Based on the proposed composition of the species from the CuO/Nb_2O_5/SiO_2-Al_2O_3 catalysts calcined at 300 °C for 6 h (Table 2), the presence of crystalline CuO and amorphous Nb_2O_5 on the surface of silica-alumina is the determining factor for optimum catalyst activity. Besides, the presence of mixed-oxide phases between Cu and Nb might be responsible for part of the active species for the observed soot oxidation.

4. Conclusion

New catalytic materials based on CuO/Nb_2O_5/SiO_2-Al_2O_3 were prepared under different methods, oxide loadings, and calcination conditions. Their characterizations indicate that the most promising materials were generated by co-impregnation of the precursors with a 1:1 CuO:Nb_2O_5 mass ratio. The active phases are very distinct, according to the loading of oxides

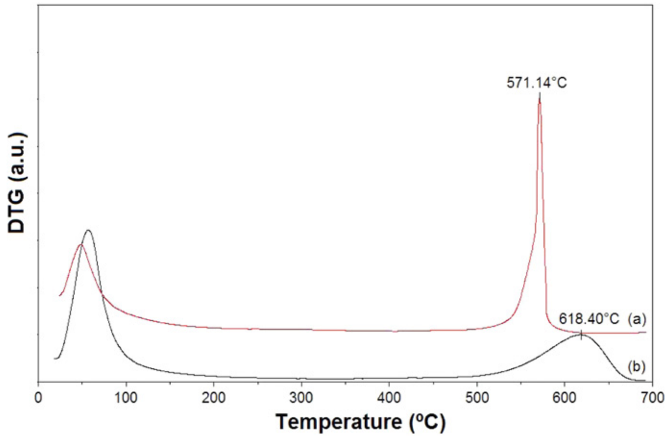

Fig. 14. DTG curves for the mixtures of 1:10 Printex® U:25 wt% CuO/SiO_2-Al_2O_3 (a) and 25 wt% Nb_2O_5/SiO_2-Al_2O_3 (b) under air at 110 mL min^{-1} and rate of 10 °C min^{-1}. The catalysts were calcined at 300 °C/6 h. Maximum temperatures (T_{ox}) are listed for each catalyst.

and calcination temperatures. At lower temperatures (300 °C for 6 h) and over 5 wt% CuO, the crystalline copper oxide predominates, whereas at higher temperatures (800 °C for 6 h) and over 10 wt% CuO, there is a mixture of the CuO, Nb_2O_5, and $CuNb_2O_6$ crystalline species. A promising application of $CuO/Nb_2O_5/SiO_2$-Al_2O_3 materials on the oxidation of diesel soot particulates was revealed by evaluating their activities by studying the thermal behavior of mixtures of catalyst and a model particulate material (Printex® U). The catalysts calcined at 300 °C for 6 h presented higher activity than those calcined at 800 °C for 6 h. The best catalyst (25 wt% CuO/25 wt% Nb_2O_5/SiO_2-Al_2O_3, calcined at 300 °C for 6 h) in the oxidation of diesel soot lowered the oxidation temperature from 622 to 518 °C.

Acknowledgments

The authors thank CNPq for a scholarship to pursue a doctorate degree (to V.S.B.) and UnB-IQ (FUNPE), FINATEC, FINEP/CTPetro, FAPDF/SCDT/CNPq, CAPES, and CNPq for financial support. The authors also thank Professor Edi Mendes Guimarães, Laboratório de Difração de Raios-X (IG/UnB), for the XRD measurements, CBMM for the niobium reagents, and Degussa for the Printex® U.

References

[1] M. Bañares, Catal. Today 51 (1999) 319.
[2] I.E. Wachs, Catal. Today 100 (2005) 79.
[3] T. Okuhara, Chem. Rev. 102 (2002) 3641.
[4] M. Ziolek, Catal. Today 78 (2003) 47.
[5] K. Tanabe, Catal. Today 78 (2003) 65.
[6] J.E. Herrera, J.H. Kwak, J.Z. Hu, Y. Wang, C.H.F. Peden, J. Macht, E. Iglesia, J. Catal. 239 (2006) 200.
[7] Y. Chen, I.E. Wachs, J. Catal. 217 (2003) 468.
[8] K. Tanabe, M. Misono, Y. Ono, H. Hattori, New Solid Acids and Bases—Their Catalytic Properties, Studies in Surface Science and Catalysis, vol. 51, Elsevier, Tokyo, 1989, p. 108.
[9] V.S. Braga, J.A. Dias, S.C.L. Dias, J.L. Macedo, Chem. Mater. 17 (2005) 690.
[10] H. Yahiro, M. Iwamoto, Appl. Catal. A 222 (2001) 163.
[11] K. Yamada, C. Pophal, K. Segawa, Microporous Mesoporous Mater. 21 (1998) 549.
[12] S. Bennice, A. Gervasini, Appl. Catal. B 62 (2006) 336.
[13] A. Gervasini, M. Manzoli, G. Marthra, A. Ponti, N. Ravasio, L. Sordelli, F. Zaccheria, J. Phys. Chem. B 110 (2006) 7851.
[14] A. Gervasini, S. Bennici, Appl. Catal. A 281 (2005) 199.
[15] S. Bennici, P. Carniti, A. Gervasini, Catal. Lett. 98 (2004) 187.
[16] S. Bennici, A. Gervasini, N. Ravasio, F. Zaccheria, J. Phys. Chem. B 107 (2003) 5168.
[17] J.W. Geus, A.J. Van Dillen, in: F.J.J. G Janssen, R.A. van Santen (Eds.), Environmental Catalysis, in: Catalytic Science Series, vol. 1, Imperial College Press, London, 1999, p. 151.
[18] S. Braum, L.G. Appel, M. Schmal, Quim. Nova 27 (2003) 472.
[19] J. Lahaye, S. Boehm, Ph. Chambrion, P. Ehrburger, Combust. Flame 104 (1996) 199.
[20] R.J. Farrauto, K.E. Voss, Appl. Catal. B 10 (1996) 29.
[21] G. Neri, G. Rizzo, S. Galvagno, A. Donato, M.G. Musolino, R. Pietropaolo, Appl. Catal. B 42 (2003) 381.
[22] D. Fino, N. Russo, E. Cauda, G. Saracco, V. Specchia, Catal. Today 114 (2006) 31.
[23] E. Aneggi, C. de Leitenburg, G. Dolcetti, A. Trovarelli, Catal. Today 114 (2006) 40.
[24] V. Serra, G. Saracco, C. Badini, V. Specchia, Appl. Catal. B 11 (1997) 329.
[25] A. Carrascull, I.D. Lick, E.N. Ponzi, M.I. Ponzi, Catal. Commun. 4 (2003) 124.
[26] H. Laversin, D. Courcot, E.A. Zhilinskaya, R. Cousin, A. Aboukais, J. Catal. 241 (2006) 456.
[27] E.I. Ko, J.G. Weissman, Catal. Today 8 (1990) 27.
[28] K. Nakamoto, Infrared Spectra of Inorganic and Coordination Compounds, second ed., Wiley–Interscience, New York, 1970, p. 244.
[29] Handbook of Chemistry and Physics, 78th ed., CRC Press, Boca Raton, FL, 1997.
[30] Ph. Galeza, J.L. Soubeyroux, Ch. Bertrand, T. Hopfinger, S. Beauquis, H. Nguyen Xuan, J. Alloys Compd. 391 (2005) 13.
[31] T. Beutel, J. Sárkany, G.-D. Lei, J.Y. Yam, W.M.H. Sachtler, J. Phys. Chem. 100 (1996) 845.
[32] T. Onfroy, G. Clet, S.B. Bukallah, D.M. Hercules, M. Houalla, Catal. Lett. 89 (2003) 15.
[33] Z. Wang, Q. Liu, J. Yu, T. Wu, G. Wang, Appl. Catal. A 239 (2003) 87.
[34] P.-O. Larsson, A. Anderssony, J. Catal. 179 (1998) 72.
[35] T. Yu, X. Zhao, Z.X. Shen, Y.H. Wu, W.H. Su, J. Cryst. Growth 268 (2004) 590.
[36] X. Gao, I.E. Wachs, M.S. Wong, J.Y. Ying, J. Catal. 203 (2001) 18.
[37] I.E. Wachs, Chem. Mater. 3 (1991) 100.
[38] J.P.A. Neeft, O.P. van Pruissen, M. Makkee, J.A. Moulijn, Appl. Catal. B 12 (1997) 21.
[39] K. Tikhomirov, O. Kröcher, M. Elsener, A. Wokaun, Appl. Catal. B 64 (2005) 72.
[40] J. van Doorn, J. Varloud, P. Mériaudeau, V. Perrichon, M. Chevrier, C. Gauthier, Appl. Catal. B 1 (1992) 117.
[41] A. Bellaloui, J. Varloud, P. Mériaudeau, V. Perrichon, E. Lox, M. Chevrier, C. Gauthier, F. Mathis, Catal. Today 29 (1996) 421.